

Supporting Information

Dual inhibition of glutaminase and carnitine palmitoyltransferase decreases growth and migration of glutaminase inhibition-resistant triple-negative breast cancer cells

Larissa Menezes dos Reis^{1,2†}, Douglas Adamoski^{1,2†}, Rodolpho Ornitiz Oliveira Souza³, Caroline Fernanda Rodrigues Ascensão^{1,2}, Krishina Ratna Sousa de Oliveira^{1,2}, Felipe Corrêa da Silva^{2,4}, Fábio Malta de Sá Patroni^{1,2}, Marília Meira Dias¹, Sílvio Roberto Consonni⁵, Pedro Manoel Mendes de Moraes Vieira⁴, Ariel Mariano Silber³, Sandra Martha Gomes Dias^{1*}

†These authors contributed equally to the work.

From the ¹Brazilian Biosciences National Laboratory (LNBio), Center for Research in Energy and Materials (CNPEM), 13083-970, Campinas, São Paulo, Brazil. ²Graduate Program in Genetics and Molecular Biology, Institute of Biology, University of Campinas- UNICAMP, Campinas, SP, Brazil. ³Department of Parasitology, Laboratory of Biochemistry of Tryps (LaBTryps), Institute of Biomedical Science, University of São Paulo - USP, 05508-000, São Paulo, SP, Brazil. ⁴Department of Genetics, Evolution, and Bioagents, Laboratory of Immunometabolism, Institute of Biology, University of Campinas-UNICAMP, 13083-970, Campinas, SP, Brazil. ⁵Department of Biochemistry and Tissue Biology, Laboratory of Citochemistry and Immunocitochemistry, Institute of Biology, University of Campinas- UNICAMP, Campinas, SP, Brazil.

Running Title: *CPT1 compensates GLS inhibition in TN breast cancer*

Figure S1

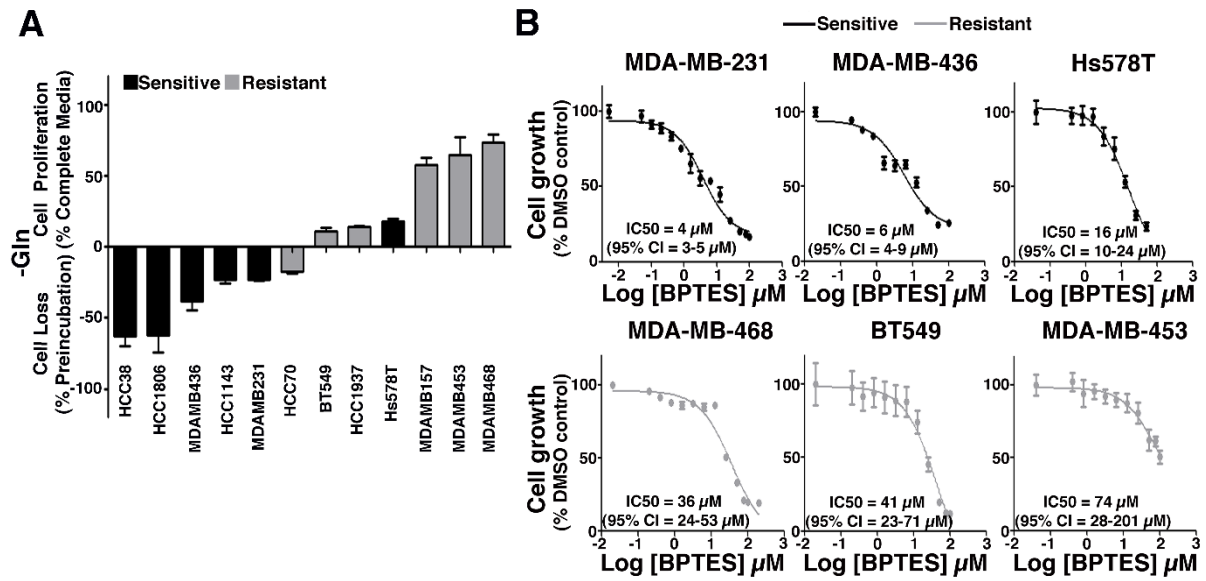


Fig. S1. TNBC cell lines have heterogeneous glutamine-withdraw sensitivity and BPTES IC₅₀ over cell growth. A, Growth response of 12 TNBC cell lines incubated with glutamine-deprived RPMI medium for 4 days. B, Growth response of 6 TNBC incubated with increasing amounts of BPTES, another glutaminase inhibitor, for 2 days. IC₅₀ value and 95% confidence interval (CI) is presented as an inset. Graphics in A-B represent the mean \pm standard deviation (SD) of n = 4.

Figure S2

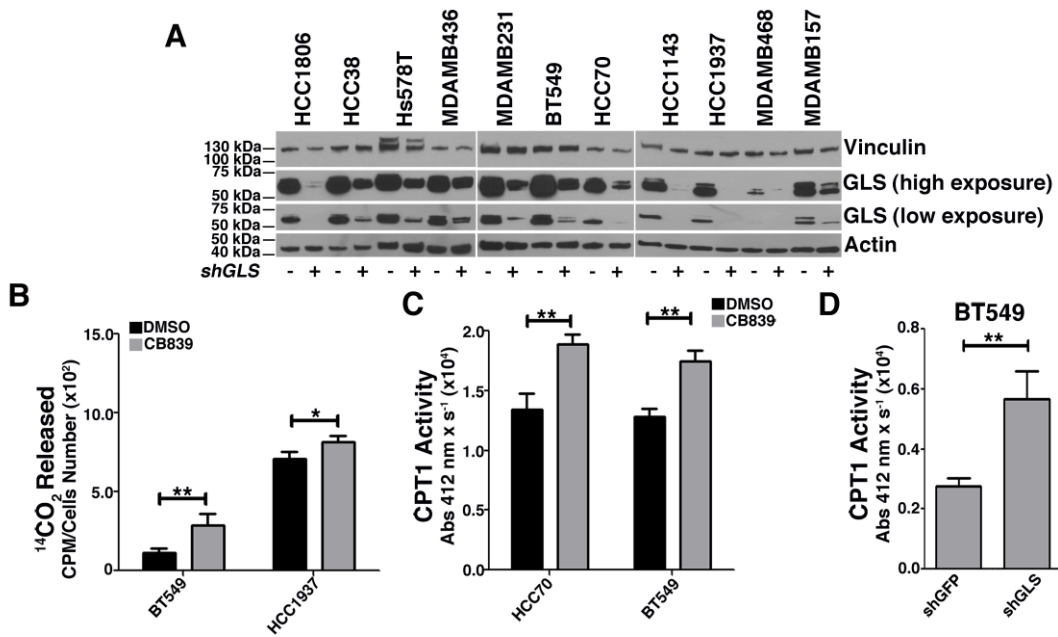


Fig. S2. Resistant cell lines respond to GLS attenuation by increasing beta-oxidation. *A*, *GLS* knockdown efficiency in 11 TNBC cell lines as shown by western blot (except MDA-MB-453). *B*, Beta-oxidation was directly measured by quantifying ¹⁴CO₂ released from uniformly labeled (¹⁴C)-palmitic acid. The resistant cell lines BT549 and HCC1937 released more ¹⁴CO₂ when treated with CB-839 compared to DMSO. *C*, CPT1 activity increase in the resistant BT549 and HCC70 cell lines after CB-839 incubation compared to DMSO. *D*, CPT1 activity increased in the resistant BT549 cell line after *GLS* knockdown. Graphics in *B-D* represent the mean ± SD of n = 3. Student t-test was applied; p < 0.05 (*), p < 0.01 (**).

Figure S3

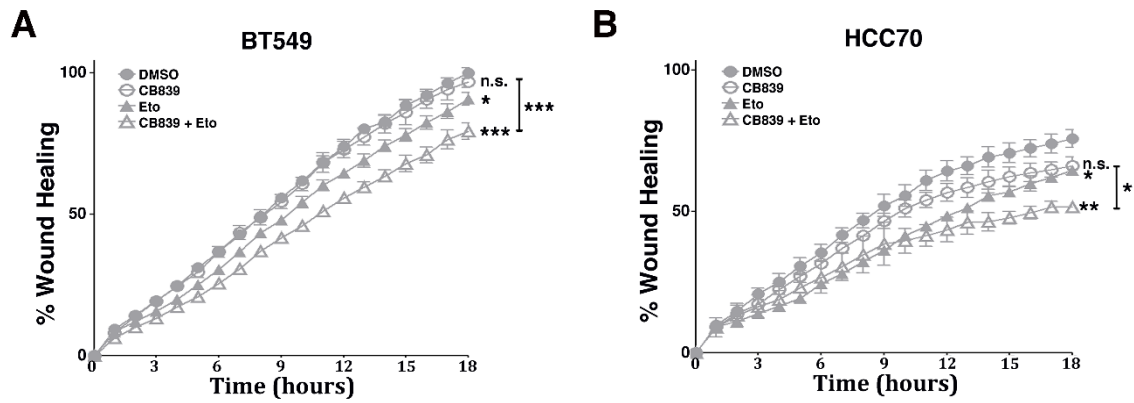


Fig. S3. Etomoxir and CB-839 combined treatment promoted a further decrease in the migration of resistant cell lines. Combined CB-839 + etomoxir treatment further decreased cell migration in the resistant BT549 (A) and HCC70 (B) cell lines compared to individual treatments. Graphics in A-B represent the mean \pm SD of $n = 4$. Student t-test was applied; $p < 0.05$ (*), $p < 0.01$ (**), $p < 0.001$ (***), n.s., non-significant. Whenever not indicated comparison was made against DMSO control.

Figure S4

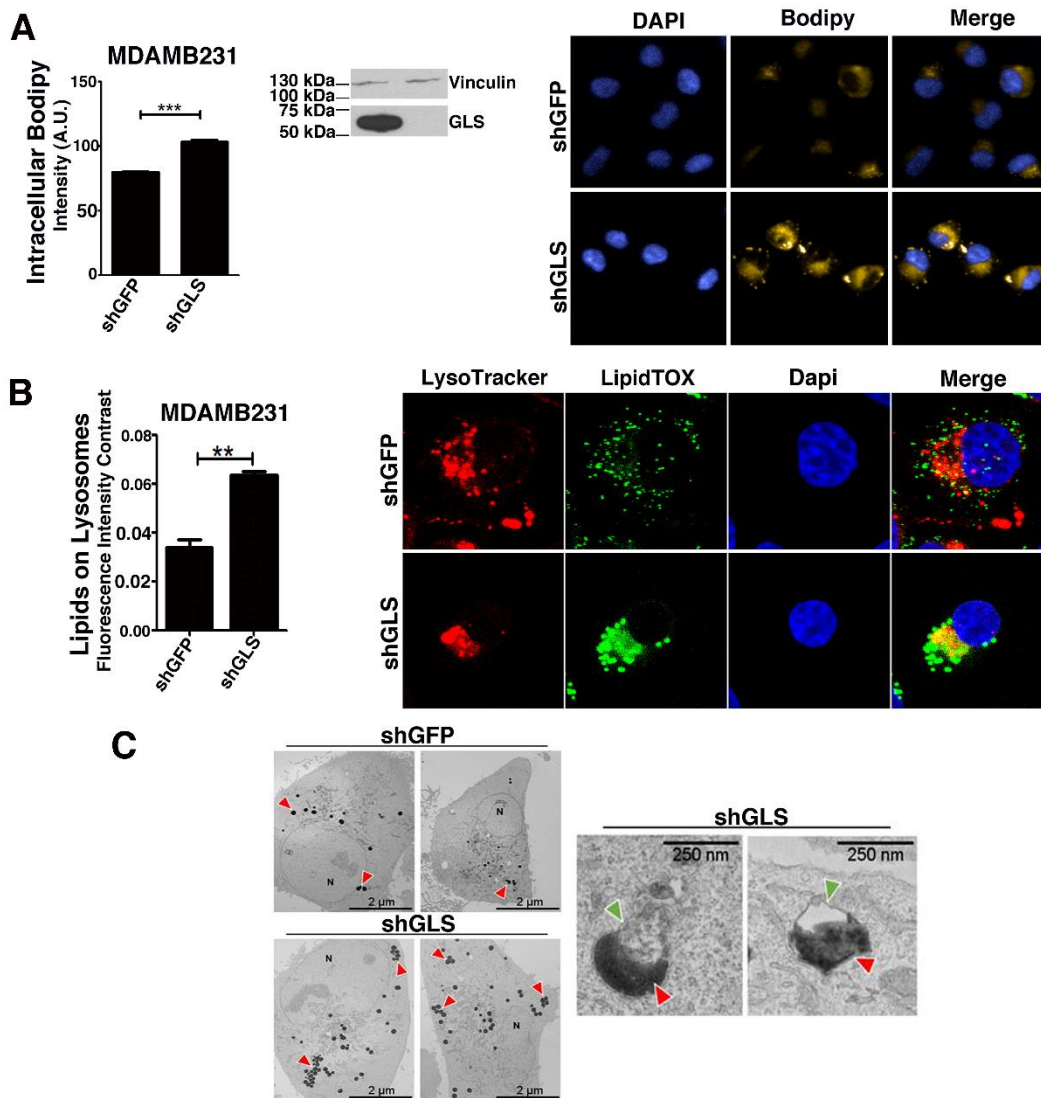


Fig. S4. MDA-MB-231 cell line responds to *GLS* knockdown by increasing FA intake and lipid droplets mobilization to lysosomes. *A*, MDA-MB-231 responded to *GLS* knockdown by capturing more C1-BODIPY 500/510 C12 fatty acid (Bodipy) from the medium. Fluorescence microscopy images on the right depicting a higher signal in cells with knocked down *GLS*. *B*, *GLS* knockdown drove cells to a higher mobilization of neutral lipid droplets (as identified by the specific marker Lipidtox) to lysosomes (stained by Lisotracker), implying lipophagy in these cells. Confocal fluorescence microscopy maximum projection images depicting lysosome and neutral lipid droplet co-staining (in yellow) in cells with *GLS* knocked down; Nuclei were stained with DAPI. *C*, On the left, transmission electron micrographs (TEM) of shGFP and shGLS cells showing a visual enrichment on lipid droplets (red arrowheads) on cells with *GLS* knocked down. N = nucleus. On the right, TEM displaying fusion between lipid droplets (red arrowheads) and autophagosomes (green arrowheads) found on shGLS cells.

Table S1. List of genes DE between resistant and sensitive cell lines and enriched pathways which are related to lipid metabolism ($\log_2 FC \geq +1$ or $\log_2 FC \leq -1$, $padj \leq 0.05$).

| GO pathway term | padj | DE genes |
|---|-------------|--|
| Lipid metabolic process GO:0006629 | 0.00008 | <i>ABCG1, ACOT1, ACSS2, ALDH1A2, ANKRD1, APOBR, CHKB-CPT1B, CISH, CLN3, CPT1B, CRAT, CYP26A1, CYP26B1, CYP27B1, DGKG, EFR3B, FGF21, GGPS1, GPC2, INPP5A, ISYNA1, OSBPL5, PAFAH2, CK2, PDSS1, PIK3C2B, PIK3R1, PLA2G3, PLA2G4B, PLA2G6, PRLR, SERINC4, SESN2, SLC16A11, SLC44A4, STARD10, SULT1E1, TBXAS1, TM7SF2, TMEM150A, TMEM86A, TRIB3, TTC39B, XBP1</i> |
| Lipid biosynthetic process GO:0008610 | 0.00120 | <i>ABCG1, ACSS2, ADGRF5, ALDH1A2, CYP27B1, GGPS1, ISYNA1, PDSS1, PIK3C2B, PIK3R1, PLA2G6, PRLR, SERINC4, TBXAS1, TM7SF2, TRIB3, XBP1</i> |
| Cellular lipid metabolic process GO:00044255 | 0.00131 | <i>ABCG1, ACSS2, ACOT1, ADGRF5, ALDH1A2, APOBR, CLN3, CPT1B, CRAT, CYP26A1, CYP26B1, EFR3B, GGPS1, GHR, GPC2, HELZ2, INPP5A, ISYNA1, PDSS1, PDPN, PIK3C2B, PIK3R1, PLA2G3, PLA2G4B, PLA2G6, SERINC4, SESN2, TBXAS1, TMEM150A, TRIB3, XBP1</i> |
| Phospholipid biosynthetic process GO:0008654 | 0.00400 | <i>ADGRF5, GGPS1, ISYNA1, PIK3C2B, PIK3R1, PLA2G6, SERINC4, XBP1</i> |
| Phospholipid metabolic process GO:0006644 | 0.00691 | <i>ADGRF5, CLN3, EFR3B, INPP5A, ISYNA1, GGPS1, PIK3C2B, PIK3R1, PLA2G3, PLA2G4B, PLA2G6, SERINC4, TMEM150A, XBP1</i> |
| Fatty acid derivative metabolic process GO:1901568 | 0.00808 | <i>ACSS3, GGTA1P, PLA2G3, PLA2G4B, TBXAS1</i> |
| Phospholipid transport GO:0015914 | 0.01141 | <i>ABCG1, ATP10A, OSBPL5</i> |
| Positive regulation of phospholipid biosynthetic process GO:0071073 | 0.01384 | <i>ADGRF5, XBP1</i> |
| Fatty acid metabolic process GO:0006631 | 0.02225 | <i>ACOT1, ACSS2, CPT1B, CRAT, GHR, PDPN, PLA2G3, PLA2G4B, SESN2, TBXAS1, TRIB3, XBP1</i> |
| Acyl carnitine transport GO:0006844 | 0.02472 | <i>CPT1B, CRAT</i> |
| Acyl carnitine transmembrane transport GO:1902616 | 0.02472 | <i>CPT1B, CRAT</i> |

| | | |
|--|---------|---|
| Cholesterol biosynthetic process GO:0045540 | 0.03002 | <i>ABCG1</i> |
| Regulation of phospholipid biosynthetic process GO:0071071 | 0.03731 | <i>ADGRF5, XBP1</i> |
| Carnitine metabolic process GO:0009437 | 0.03967 | <i>CPT1B, CRAT</i> |
| Unsaturated fatty acid metabolic process GO:0033559 | 0.04735 | <i>PDPN, PLA2G4B, TBXAS1</i> |
| Lipid transport GO:0006869 | 0.04841 | <i>ABCG1, APOBR, ATP10A, CPT1B, DISP3, OSBPL5, PLA2G6, SLCO2A1, STARD10, FZD4</i> |

Table S2. List of genes DE between resistant and sensitive cell lines, which were related to the pathways listed in Table S1. Genes related to beta-oxidation and lipid catabolism are in bold.

| Gene | log2(FC) (Resistant/Sensitive) | padj | Gene | log2(FC) (Resistant/Sensitive) | padj |
|-----------------------|-----------------------------------|----------|--------------------------|-----------------------------------|----------|
| <i>ATP10A</i> | -5.14 | 3.3E-12 | <i>TM7SF2</i> | 2.24 | 0.010333 |
| <i>IGFBP1</i> | -4.32 | 0.001869 | <i>ISYNA1</i> | 2.28 | 0.012792 |
| <i>PDPN</i> | -4.03 | 0.005988 | <i>EFR3B</i> | 2.28 | 0.023631 |
| <i>ANKRD1</i> | -3.84 | 0.004141 | <i>PLA2G6</i> | 2.28 | 0.007354 |
| <i>ADGRF5</i> | -3.72 | 0.009985 | <i>SERINC4</i> | 2.39 | 0.033476 |
| <i>DGKG</i> | -3.45 | 0.018184 | <i>CHKB-CPT1B</i> | 2.39 | 0.009758 |
| <i>CYP26A1</i> | -3.01 | 0.035812 | <i>GPC2</i> | 2.40 | 0.004141 |
| <i>ACSS3</i> | -2.95 | 0.031423 | <i>APOBR</i> | 2.40 | 0.035456 |
| <i>TBXAS1</i> | -2.25 | 0.005988 | <i>CYP27B1</i> | 2.40 | 0.017153 |
| <i>CYP26B1</i> | -2.05 | 0.028926 | <i>CRAT</i> | 2.46 | 0.026845 |
| <i>PDSS1</i> | -1.46 | 0.002857 | <i>OSBPL5</i> | 2.47 | 0.0052 |
| <i>INPP5A</i> | -1.40 | 0.004229 | <i>SLC16A11</i> | 2.57 | 0.040341 |
| <i>PAFAH2</i> | 1.02 | 0.003687 | <i>TMEM86A</i> | 2.59 | 0.022815 |
| <i>ACSS2</i> | 1.13 | 0.044733 | <i>PRLR</i> | 2.62 | 0.013213 |
| <i>GGPS1</i> | 1.24 | 0.025419 | <i>STARD10</i> | 2.71 | 0.004409 |
| <i>ACOT1</i> | 1.40 | 0.031423 | <i>GNA14</i> | 2.78 | 0.045759 |
| <i>CLN3</i> | 1.51 | 0.014323 | <i>FGF21</i> | 2.85 | 0.045759 |
| <i>TMEM150A</i> | 1.56 | 0.030933 | <i>CISH</i> | 2.86 | 0.003657 |
| <i>FZD4</i> | 1.58 | 0.033288 | <i>XBPI</i> | 2.86 | 0.000323 |
| <i>SESN2</i> | 1.60 | 0.026989 | <i>CREB3L4</i> | 3.02 | 0.000323 |
| <i>CPT1B</i> | 1.68 | 0.049406 | <i>SLCO2A1</i> | 3.06 | 0.008565 |
| <i>PIK3C2B</i> | 1.73 | 0.046818 | <i>ABCG1</i> | 3.25 | 0.010536 |
| <i>HELZ2</i> | 1.82 | 0.04533 | <i>GHR</i> | 3.30 | 0.028926 |
| <i>TTC39B</i> | 1.89 | 0.043085 | <i>DISP3</i> | 3.37 | 0.00075 |
| <i>TRIB3</i> | 1.95 | 0.013852 | <i>PLA2G3</i> | 3.90 | 0.003395 |
| <i>PIK3R1</i> | 1.95 | 0.003009 | <i>SULT1E1</i> | 3.92 | 0.002022 |
| <i>PLA2G4B</i> | 2.02 | 0.047481 | <i>ALDH1A2</i> | 3.98 | 0.00103 |
| <i>PCK2</i> | 2.18 | 0.000678 | <i>SLC44A4</i> | 4.40 | 0.000433 |

Table S3. List of genes DE between low and high *GLS* breast tumors related to the “fatty acid oxidation process” (intersection between GO #0006631 and GO # 0019395).

| GeneSymbol | log2FC (low/high) | padj | GeneSymbol | log2FC (low/high) | padj |
|----------------|----------------------|----------|-----------------|----------------------|----------|
| <i>SLC27A2</i> | 2.69 | 2.88E-31 | <i>SCP2</i> | 0.42 | 7.24E-07 |
| <i>ACOX2</i> | 2.67 | 2E-36 | <i>ADIPOR1</i> | 0.42 | 4.95E-09 |
| <i>PLIN5</i> | 2.48 | 1.54E-26 | <i>ETFDH</i> | 0.39 | 1.25E-08 |
| <i>ACSM1</i> | 2.14 | 6.77E-36 | <i>ACOT8</i> | 0.37 | 7.11E-06 |
| <i>CRAT</i> | 2.10 | 1.73E-36 | <i>AUH</i> | 0.34 | 4.23E-06 |
| <i>ECI1</i> | 1.47 | 1.1E-45 | <i>CPT1B</i> | 0.33 | 0.012091 |
| <i>IVD</i> | 1.35 | 2.33E-47 | <i>ACAT1</i> | 0.33 | 0.001647 |
| <i>ECI2</i> | 1.32 | 1.01E-27 | <i>AKT2</i> | 0.33 | 3.62E-07 |
| <i>DECR2</i> | 1.22 | 2.92E-29 | <i>HADH</i> | 0.31 | 0.000157 |
| <i>ACADS</i> | 1.18 | 3.16E-19 | <i>HACL1</i> | 0.23 | 0.001316 |
| <i>CROT</i> | 1.16 | 1.11E-16 | <i>PECR</i> | 0.21 | 0.035404 |
| <i>ETFB</i> | 0.95 | 1.9E-10 | <i>PEX2</i> | 0.18 | 0.008166 |
| <i>PEX7</i> | 0.86 | 3.59E-26 | <i>SLC25A17</i> | 0.17 | 0.012334 |
| <i>ECHDC2</i> | 0.80 | 5.19E-14 | <i>MLYCD</i> | 0.17 | 0.029296 |
| <i>ADIPOR2</i> | 0.79 | 8.96E-13 | <i>MTOR</i> | -0.19 | 0.008311 |
| <i>ACOX3</i> | 0.76 | 3.97E-16 | <i>ACOX1</i> | -0.24 | 0.003667 |
| <i>AMACR</i> | 0.76 | 8.54E-16 | <i>HIBCH</i> | -0.32 | 0.000182 |
| <i>CPT1A</i> | 0.75 | 2.53E-09 | <i>PHYH</i> | -0.32 | 0.006093 |
| <i>ECH1</i> | 0.75 | 1.23E-15 | <i>PEX13</i> | -0.34 | 4.51E-07 |
| <i>ECHS1</i> | 0.74 | 1.94E-17 | <i>EHHADH</i> | -0.35 | 0.003127 |
| <i>HSD17B4</i> | 0.74 | 6.41E-15 | <i>PPARD</i> | -0.36 | 1.26E-05 |
| <i>IRS1</i> | 0.73 | 5.13E-06 | <i>PRKAG2</i> | -0.39 | 5.09E-07 |
| <i>ACAA1</i> | 0.72 | 3.6E-18 | <i>MAPK14</i> | -0.42 | 1.59E-12 |
| <i>ALDH3A2</i> | 0.71 | 1.2E-08 | <i>ABCD1</i> | -0.42 | 0.000509 |
| <i>ETFBKMT</i> | 0.66 | 8.34E-14 | <i>ACAT2</i> | -0.43 | 0.000287 |
| <i>TYSND1</i> | 0.65 | 9.82E-16 | <i>ACAA2</i> | -0.44 | 1.81E-05 |
| <i>ABCD3</i> | 0.63 | 6.24E-11 | <i>PRKAA1</i> | -0.59 | 1.59E-08 |
| <i>ACACB</i> | 0.60 | 4.23E-05 | <i>ACAD11</i> | -0.70 | 1.48E-08 |
| <i>APPL2</i> | 0.60 | 1.63E-14 | <i>ECHDC1</i> | -0.81 | 2.78E-13 |
| <i>AKT1</i> | 0.58 | 1.27E-13 | <i>ALOX12</i> | -0.88 | 4.04E-09 |
| <i>ACAD10</i> | 0.55 | 2.31E-17 | <i>NR4A3</i> | -1.16 | 3.17E-11 |
| <i>ACOXL</i> | 0.55 | 0.006364 | <i>DGAT2</i> | -1.20 | 2.09E-13 |
| <i>ACADVL</i> | 0.54 | 7.56E-10 | <i>ADH7</i> | -1.46 | 0.011757 |
| <i>LONP2</i> | 0.53 | 2.13E-09 | <i>PPARA</i> | -1.62 | 1.31E-52 |
| <i>CPT2</i> | 0.48 | 1.57E-12 | <i>ABCD2</i> | -2.25 | 2.43E-36 |
| <i>GCDH</i> | 0.48 | 6.12E-08 | <i>PPARGC1A</i> | -2.64 | 1.45E-24 |
| <i>SESN2</i> | 0.47 | 1.06E-06 | <i>HAO1</i> | -6.64 | 1.97E-54 |
| <i>MCAT</i> | 0.43 | 8.8E-07 | | | |